Dental Materials Journal 2019; 38(3): 444–451

Cortical bone response toward nanosecond-pulsed laser-treated zirconia implant surfaces

Masatsugu HIROTA[1], Tomohiro HARAI[2], Shinji ISHIBASHI[2], Masayoshi MIZUTANI[2] and Tohru HAYAKAWA[1]

[1] *Department of Dental Engineering, Tsurumi University School of Dental Medicine, 2-1-3 Tsurumi, Tsurumi-ku, Yokohama, Kanagawa 230-8501, Japan*

[2] *Department of Mechanical Systems Engineering, Graduate School of Engineering, Tohoku University, 6-6-01 Aoba, Aramaki, Aoba-ku, Sendai, Miyagi 980-8579, Japan*

Corresponding author, Masatsugu HIROTA; E-mail: hirota-masatsugu@tsurumi-u.ac.jp

Two type of partially stabilized zirconia, namely yttria-stabilized tetragonal zirconia polycrystals (Y-TZP) and ceria-stabilized tetragonal zirconia polycrystals including aluminum oxide nanocomposite (Ce-TZP), were irradiated by nanosecond-pulsed Nd:YAG laser and the regular structure with concave and convex of each 30 μm width and 30 μm depth were prepared on both surfaces. In the case of Ce-TZP, the surface was changed to be black after laser irradiation. EDX measurement revealed the reduction of more amounts of oxygen atoms on Ce-TZP compared to Y-TZP. Laser irradiated zirconia implants were inserted into the bone defects of rat femur during 4 weeks. As a control, large grid sandblasted and acid etching (blastedHF) implant was used. Laser treatment for Y-TZP provided greater degree of bone-implant contact ratio than blastedHF treated Y-TZP ($p<0.05$). In the case of Ce-TZP, however, laser treatment showed no clear effect on bone response.

Keywords: Zirconia implant, Nanosecond-pulsed laser, Osseointegration, Osteoblast, Bone-to-implant contact

INTRODUCTION

In recent years, high-strength partially stabilized zirconia implants have attracted attention as an alternative to titanium implants[1-4]. Yttria-stabilized tetragonal zirconia polycrystals (Y-TZP) is a partially-stabilized zirconia and has superior mechanical properties such as high fracture toughness in addition to better esthetic properties. Y-TZP is expected to address the shortcoming of titanium implants such as their dark-grayish color[5] and metal sensitivity[6].

To improve the bone-tissue response of zirconia implants, some surface modifications have been reported including hydroxyapatite coating[7], ultraviolet irradiation[8], sandblasting[9] and acid etching[10]. The combination of large-grid sandblasting and hydrofluoric acid etching treatment (abbreviated as blastedHF) of zirconia surfaces produced micro- and nano-topographies and improved the proliferation and differentiation activities of osteoblast-like cells or mesenchymal stem cells[11,12].

Laser treatment is a useful method for creating micro- and nano-scale rough surfaces. Delgado-Ruíz *et al.*[13] reported that the application of a femtosecond laser created microgrooves of 30 μm width and 70 μm pitch on a zirconia surface. Higher bone-to-implant contact (BIC) and higher peripheral bone density were obtained for femtosecond laser treated zirconia after immediate loading compared with sand-blasted and acid-etched titanium when implanted into the edentulous lower jaws of foxhound dogs[14]. Their report also showed that the zirconia implants with microgrooves can osseointegrate better than titanium implants in terms of BIC and crystal bone resorption at 1 and 3 months after implantation.

Surface chemistry is also an important factor in controlling bone response, in addition to the surface morphology. Nanosecond-pulse laser irradiation can alter not only the surface morphology and roughness but also the condition of the titanium oxide layer by heat input, resulting in better cytocompatibility[15,16]. Fukayo *et al.*[17] evaluated tissue response towards nanosecond-pulsed laser-treated titanium after implantation into the tibiae of rabbits or the extracted sockets of rat maxillary molars. They found that nanosecond-pulsed laser treatment resulted in improved bone responses and attachment of gingival connective tissue.

Besides Y-TZP, ceria-stabilized tetragonal zirconia polycrystals including aluminum oxide nanocomposite (Ce-TZP) has been developed[18,19]. Al_2O_3 nanoparticles are dispersed among ceria-stabilized tetragonal zirconia polycrystals granules. Ce-TZP is reported to have higher resistance to low-temperature degradation than Y-TZP[20].

In the present study, we aimed to apply nanosecond-pulsed laser processing for zirconia surface treatment and evaluated the bone response after implantation into bone defects of rats. The effect of laser treatment on bone response was compared with blastedHF treatment. Two types of zirconia, Y-TZP and Ce-TZP, were employed. The null hypothesis tested was that nanosecond-pulsed laser treatment improves bone response compared with blastedHF treatment and that the difference among zirconia, Y-TZP and Ce-TZP, does not influence the bone response.

Received May 8, 2018: Accepted Sep 12, 2018
doi:10.4012/dmj.2018-153 JOI JST.JSTAGE/dmj/2018-153

Table 1 Conditions of laser treatment for Y-TZP and Ce-TZP implants

Parameter	laser/Y-TZP and laser/Ce-TZP implants
Pulse length	3 ns
Pulse energy	150 μJ/pulse
Wave length	1,064 nm
Frequency	50 Hz
Feed speed	7 μm/s
Laser spot	Top hat, 30×60 μm
Atmosphere	In air

MATERIALS AND METHODS

Implant material and nanosecond-pulsed laser surface treated implants

In this study, two kinds of partially stabilized zirconia were used. Yttria (3 mol Y_2O_3) stabilized tetragonal zirconia polycrystals (Y-TZP, TZ-3YB-E, Tosoh, Tokyo, Japan) and ceria (10 mol CeO_2) stabilized tetragonal zirconia polycrystals including 30 vol% Al_2O_3 (Ce-TZP, NANOZR, Panasonic Healthcare, Ehime, Japan) were fabricated as rectangular plates (3 mm in length, 2 mm in width and 1 mm in height). The plate surfaces were polished with #1200 waterproof paper under running water.

After polishing, the zirconia specimens were divided into blastedHF treatment and laser treatment groups. For blastedHF treatment, sandblasting was performed perpendicularly to the zirconia surface from a distance of 20 mm with 200 μm alumina particles at 0.5 MPa air pressure, and acid etching was carried out on the blasted surface with 46% hydrofluoric acid (HF) for 15 min at room temperature[21].

For laser treatment, each zirconia surface was treated with a Nd:YAG nanosecond-pulsed laser in a striped pattern as described in previous reports[15,16]. The processing parameters for laser treatment are listed in Table 1. Laser treatment was applied perpendicular to the substrate onto any one side.

BlastedHF treatment was performed on both sides of zirconia specimens due to the difficulties of single-side HF etching. Laser treatment was performed on one side of zirconia specimens. BlastedHF and laser treated zirconia plates were then cleaned with an ultrasonic cleaner (VS-100III, AS ONE, Osaka, Japan) using ethanol and distilled water for 20 min. Prior to implantation, the specimens were sterilized using an autoclave (Sterilizer LISA, W&H Sterilization, Brusaporto, Italy). Thus, four types of zirconia specimens —blastedHF treated Y-TZP (blastedHF/Y-TZP), laser treated Y-TZP (laser/Y-TZP), blastedHF treated Ce-TZP (blastedHF/Ce-TZP), and laser treated Ce-TZP (laser/Ce-TZP)— were obtained.

Surface analysis

The surfaces of blastedHF/Y-TZP, laser/Y-TZP, blastedHF/Ce-TZP, and laser/Ce-TZP were observed by scanning electron microscope (SEM; SU1510, Hitachi High-Technologies, Tokyo, Japan). The samples of laser/Y-TZP and laser/Ce-TZP were cut vertically with a diamond saw and the cross-sectional specimens were polished using #2000 emery paper under running water. Afterwards, cross-sectional views of laser-irradiated specimens were also observed by SEM.

Each specimen surface before and after laser irradiation was analyzed by energy dispersive X-ray spectroscopy (EDX; EMAX x-act, HORIBA, Kyoto, Japan) at accelerating voltage of 15 kV. The analyzed area was set within 30 μm width and 80 μm height onto convex and concave areas.

Animal experiment

The animal experiment was approved by the Animal Experimental Ethical Guidelines of Tsurumi University School of Dental Medicine (certificate no. 28A042). A total of 12 male Wistar rats, each weighing approximately 180 g and at 6 weeks of age, were used. The rats were housed two per cage at 20–25°C in a 12 h circadian light rhythm environment and fed water and food *ad libitum* during the experimental period.

Each zirconia implant was placed in a femur bone defect according to the previously-described procedure[22]. Each rat received one implant. A total of 12 implants, namely 3 laser/Y-TZP, 3 laser/Ce-TZP, 3 blastedHF/Y-TZP and 3 blastedHF/Ce-TZP implants, were inserted for 4-week implantation periods.

Surgery was performed under general inhalation anesthesia with a 4% isoflurane and oxygen mixture, which was reduced to 2% isoflurane during surgical manipulation. After shaving the hind limb and disinfecting the operating field, xylocaine was injected as local anesthesia. A longitudinal incision was made on the distal surface of the hind limb to expose the femur. A cortical bone defect measuring 1.0×2.0 mm was created through the cortex and the medulla. The bone defect was prepared with a very gentle surgical technique and continuous internal cooling with physiological saline solution. After press-fitting an implant into the bone defect, muscle tissue and skin were closed in separate layers using non-absorbable sutures. A prophylactic

antibiotic equivalent to latamoxef sodium (0.01 mg/kg Shimalin, Shionogi, Osaka, Japan) was administered to prevent infection.

Bone labeling was performed by fluorochrome administration using two kinds of reagent. All rats were injected with 50 mg/kg xylenol orange (Dojindo, Tokyo, Japan) by subcutaneous infusion to the back at 2 weeks after implantation. In addition, 15 mg/kg calcein (Dojindo) was injected at 3 weeks after implantation. Rats were sacrificed at 4 weeks after implantation by a peritoneal injection of an overdose of thiamylal sodium (Isothol, Nichi-Iko Pharmaceutical, Toyama, Japan). The implants and surrounding femoral bone were harvested.

Histological and histomorphometrical observations

After removing the surrounding tissue, specimens were fixed in 15% neutral buffered formalin solution (pH 7.4), dehydrated through a graded series of ethanol and then embedded in methylmethacrylate. Non-decalcified thin sections with a thickness of approximately 50–70 mm were made in a direction perpendicular to the axis of the implants using a cutting-grinding technique (EXAKT-Cutting Grinding System, BS-300CP band system & 400 CS microgrinding system, EXAKT, Norderstedt, Germany)[23].

Fluorochrome labeling by xylenol orange and calcein was evaluated using a confocal laser-scanning microscope (CLSM; TCS Multi-Photon, Leica, Germany) before staining. Regions of interest (ROI) for quantitative analysis were determined as illustrated in Fig. 1. ROI was set on both sides for blastedHF samples. For laser irradiated samples, ROI was set only one side irradiated with laser. The total length of xylenol orange and that of calcein labels per ROI area on CLSM images was determined using an image analysis system (WinROOF, Visual System Division Mitani, Tokyo, Japan).

Sections were then stained with methylene blue and basic fuchsin and were histologically evaluated using a light microscope (Eclipse Ni, Nikon, Tokyo, Japan, magnification ×40, ×100, ×400). As well as a descriptive evaluation, histomorphometrical analysis was performed as described previously[22]. The bone-to-implant contact ratio (BIC) and bone mass (BM) around the implant in decalcified stained sections were measured using an image analysis system. BIC was calculated as the percentage of the length of bone-implant contact within the ROI. BM was defined as the percentage of newly-formed bone within the ROI.

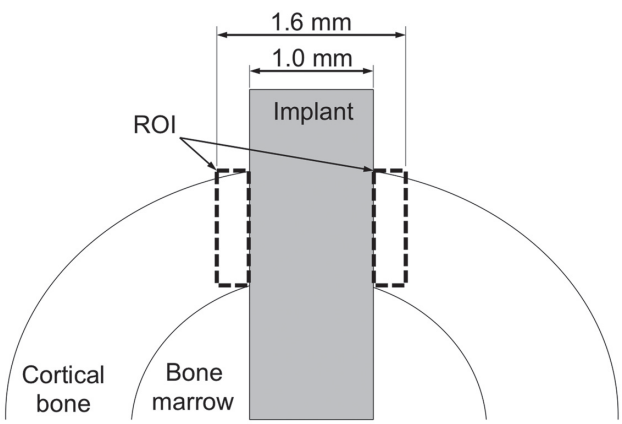

Fig. 1 Schematic drawing of the region of interest (ROI).

Statistical analysis

The results of length of fluorescence labeling, BIC and BM from histomorphometrical measurements were evaluated by a one-way analysis of variance (ANOVA) and the Bonferroni test for multiple comparisons among the means at p=0.05 with Origin Pro 9.0 J (OriginLab, Northampton, MA, USA).

RESULTS

SEM observation of SLA and laser-treated surfaces

Figure 2 shows SEM pictures of the surfaces of blastedHF/Y-TZP and blastedHF/Ce-TZP. Higher magnification images confirmed the nanoscale-roughening of both surfaces. The roughened boundaries were more clearly observed for blastedHF/Ce-TZP. Some cubic structures were present on blastedHF/Y-TZP.

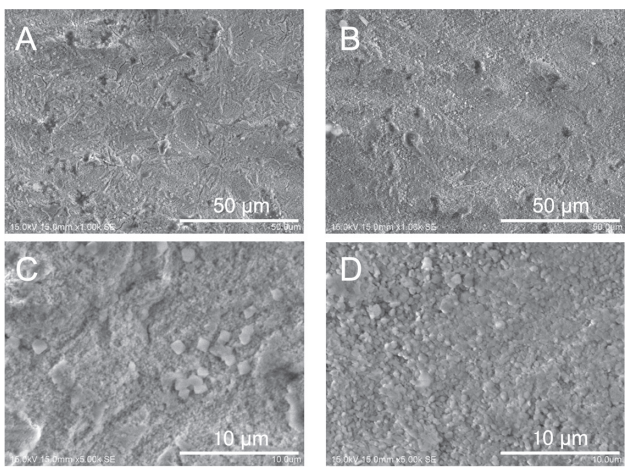

Fig. 2 SEM pictures of the surfaces of blastedHF/Y-TZP and blastedHF/Ce-TZP implants.
(A), (C) blastedHF/Y-TZP, (B), (D) blastedHF/Ce-TZP.

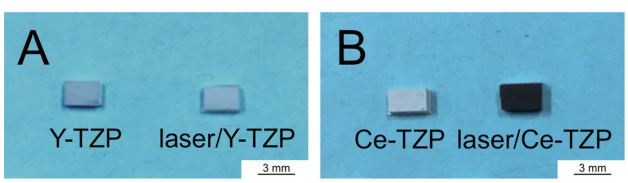

Fig. 3 Macroscopic appearances of Y-TZP, Ce-TZP, laser/Y-TZP and laser/Ce-TZP implants.
(A) Y-TZP substrate, (B) Ce-TZP substrate.

Figure 3 shows the macroscopic appearances of Y-TZP, Ce-TZP, laser/Y-TZP and laser/Ce-TZP implants. After laser irradiation, the surface of Ce-TZP became black. Y-TZP showed almost no color change after laser irradiation. No cracks were found on the surfaces of either laser/Y-TZP or laser/Ce-TZP. Figure 4 shows SEM images of the surfaces of laser/Y-TZP and laser/Ce-TZP implants. Parallel groves were produced by the laser irradiation. Regular structures with 60 μm pitch of concave and convex stripes each 30 μm in width were clearly observed on the surfaces of laser/Y-TZP and laser/Ce-TZP. The inside surface of microgrooves was roughened, and the presence of asperities was recognized in the microgrooves. The asperities were approximately 1 μm in size in laser/Y-TZP and 4 μm in laser/Ce-TZP. Figure 5 shows SEM images of the cross-sectional views of laser/Y-TZP and laser/Ce-TZP implants. Regular patterns were identified, and the depth of microgrooves was approximately 30 μm for both laser/Y-TZP and laser/Ce-TZP.

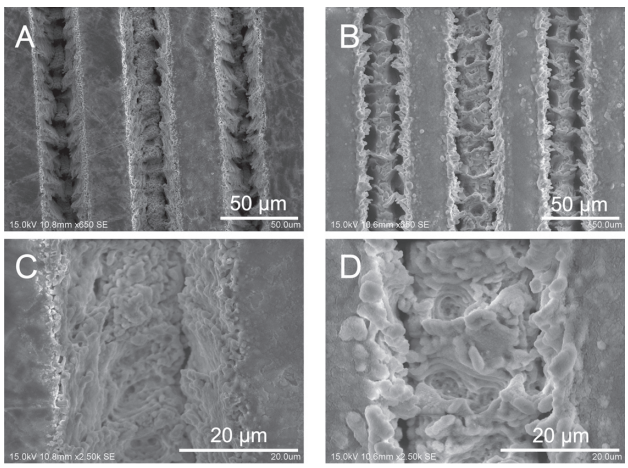

Fig. 4 SEM images of the surfaces of laser/Y-TZP and laser/Ce-TZP implants.
(A), (C) laser/Y-TZP, (B), (D) laser/Ce-TZP.

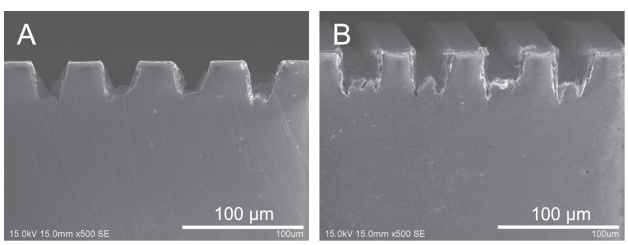

Fig. 5 SEM images of the cross-sectional observation of laser/Y-TZP and laser/Ce-TZP implants.
(A) laser/Y-TZP, (B) laser/Ce-TZP.

EDX measurement

Table 2 shows the results of EDX measurement of each specimen. The reduction of oxygen both before and after laser irradiation at the convex/concave area was confirmed by EDX in both Y-TZP and Ce-TZP. In particular, greater oxygen decrease was seen in laser/Ce-TZP compared with laser/Y-TZP.

Histological and histomorphometrical evaluations

Rats remained in good health during the experimental period. No clinical signs of inflammation or adverse tissue reactions were observed when animals were sacrificed, and all implants were still *in situ*.

Figure 6 shows CLSM pictures of blastedHF/Y-TZP and laser/Y-TZP and those of blastedHF/Ce-YZP and laser/Ce-TZP implants. New bone formation at 2 weeks after implantation was indicated as orange labeling by xylenol orange and the bone formation at 3 weeks after implantation was indicated as green labeling by calcein. New bone formation was observed in a vertical direction towards the microgrooved surfaces of laser/Y-TZP and laser/Ce-TZP. In contrast, random orientation of bone formation was recognized close to the surfaces of blastedHF/Y-TZP and blastedHF/Ce-TZP. The lengths of fluorescence labeling by xylenol orange and calcein in the ROI are shown in Table 3. No significant differences were obtained among four different groups.

Table 2 EDX measurements of Y-TZP and laser/Y-TZP, and Ce-TZP and laser/Ce-TZP

Specimens	Elements	Before laser irradiation		After laser irradiation			
				Convex area		Concave area	
		Atomic%	Weight%	Atomic%	Weight%	Atomic%	Weight%
laser/Y-TZP	C	10.28	20.84	12.43	30.67	10.64	26.4
	O	43.98	66.95	26.9	49.84	28.89	53.84
	Zr	45.75	12.21	59.27	19.26	60.47	19.76
laser/Ce-TZP	C	7.09	11.88	13.92	30.13	12.8	28.79
	O	61	76.7	30.13	48.95	29.55	49.89
	Al	8.34	6.22	8.48	8.17	7.43	7.44
	Zr	23.57	5.2	39.67	11.3	40.53	12
	Ce	—	—	7.79	1.45	9.69	1.87

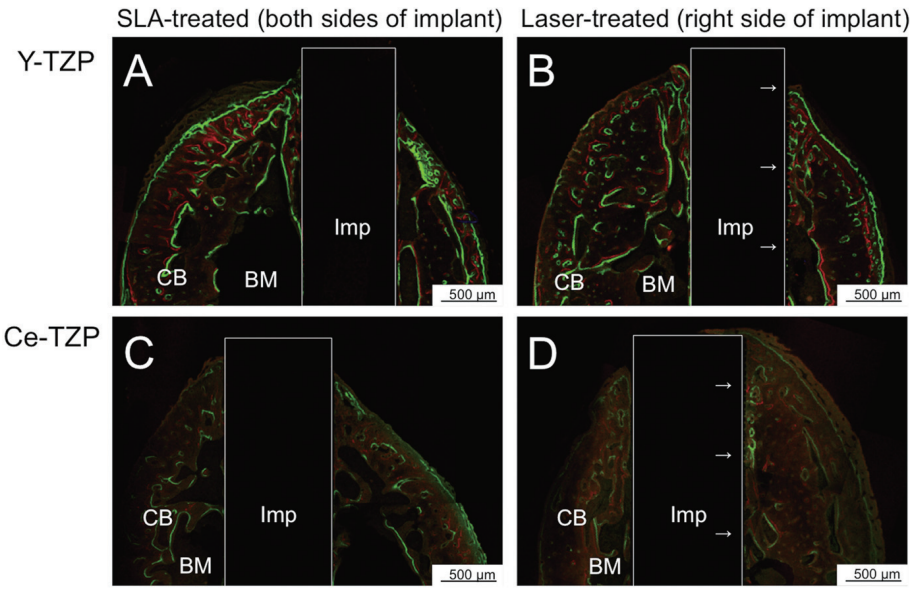

Fig. 6 CLSM pictures of blastedHF/Y-TZP, laser/Y-TZP, blastedHF/Ce-TZP and laser/Ce-TZP implants in the femur.
Orange labeling: administration of xylenol orange at 2 weeks after implantation. Green labeling: administration of calcein at 3 weeks after implantation. (A) blastedHF /Y-TZP implants (B) laser/Y-TZP implants (C) blastedHF /Ce-TZP implants (D) laser/Ce-TZP implants. Imp and white line: Implant. CB: Cortical Bone. BM: Bone Marrow. Arrows: Laser treated side.

Table 3 Length of fluorescence labeling

Specimen	Length of fluorescence labeling (mm)	
	Xyleno orange labeled	Calcein labeled
laser/Y-TZP	1.74 (0.44)	2.21 (1.33)
blastedHF/Y-TZP	1.47 (0.47)	2.31 (0.68)
laser/Ce-TZP	1.72 (0.94)	2.29 (0.86)
blastedHF/Ce-TZP	1.29 (0.52)	1.89 (0.61)

Values in brackets are SD. There were no significant differences between the groups.

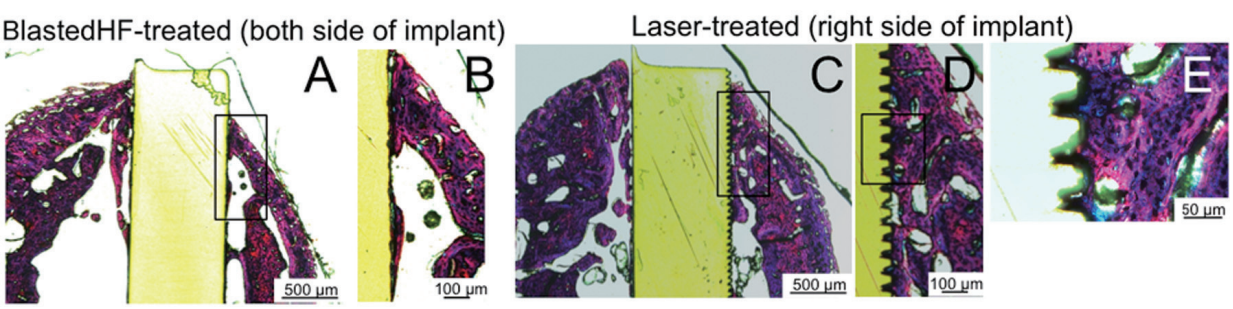

Fig. 7 Histological appearances of implants 4 weeks after their implantation into rat femur bone defects.
(A), (B) blastedHF/Y-TZP implants (C), (D), (E) laser/Y-TZP implants (A, C: magnification ×40, B, D: magnification ×100, E: magnification ×400). (B) and (D) are higher magnification images of boxed area of (A) and (C), respectively. (E) is more high magnification images of boxed are of (D).

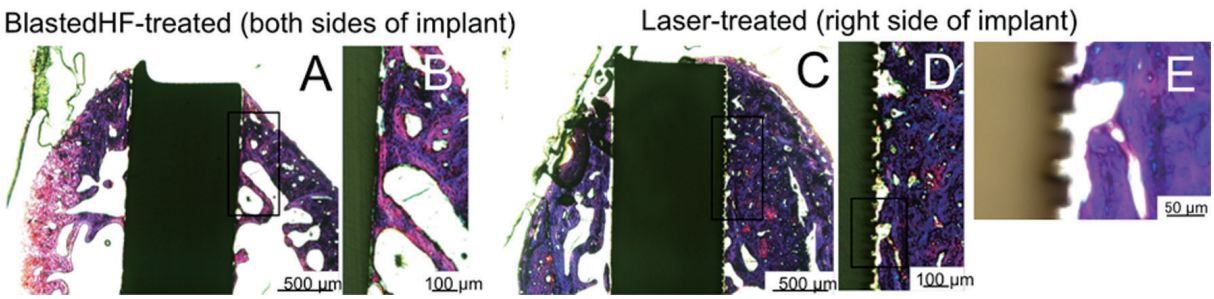

Fig. 8 Histological appearances of implants 4 weeks after their implantation into bone defects in the rat femur. (A), (B) blastedHF/Ce-TZP implants (C), (D), (E) laser/Ce-TPZ implants (A, C: magnification ×40, B, D: magnification ×100, E: magnification ×400). (B) and (D) are higher magnification images of boxed area of (A) and (C), respectively. (E) is more high magnification images of boxed are of (D).

Table 4 Percentage of the measured BIC and BM

Specimen	BIC (%)	BM (%)
laser/Y-TZP	78.9 (6.57)	72.4 (10.60)[b]
blastedHF/Y-TZP	56.2 (3.56)[a]	58.0 (6.79)[b]
laser/Ce-TZP	14.0 (2.43)	68.0 (13.35)[b]
blastedHF/Ce-TZP	37.1 (14.01)[a]	53.7 (6.44)[b]

Values in brackets are SD.
[a, b] Significantly different at $p>0.05$

Figures 7 and 8 show the histological appearances of blastedHF/Y-TZP and laser/Y-TZP and those of blastedHF/Ce-TZP and laser/Ce-TZP implants. Higher magnification images of boxed area for each specimen are also shown. For laser/Y-TZP and laser/Ce-TZP, more high images are added. Permeation of inflammatory cells was not observed. New bone formation was observed around implants after 4 weeks of implantation. Bone remodeling proceeded and mature bone formation was detected. Tight bone-to-implant bonding was observed for blastedHF/Y-TZP and laser/Y-TZP implants. Some gaps were present between bone and blastedHF/Ce-TZP and laser/Ce-TZP implants. In particular, laser/Ce-TZP showed more gaps between bone and the implant surface.

Table 4 shows the percentages of BIC and BM after 4 weeks of implantation. BIC of laser/Y-TZP implants was significantly the highest among the four different implants ($p<0.05$). No significant differences were recognized between blastedHF/Y-TZP and blastedHF/Ce-TZP ($p>0.05$). Laser/Ce-TZP significantly showed the lowest BIC ($p<0.05$). Regarding BM, there were no significant differences among the four different groups ($p>0.05$).

DISCUSSION

In the present study, we evaluated the bone responses of nanosecond-pulsed laser treated zirconia implants by comparing with blastedHF treated zirconia implants. Implants were inserted into rat femur bone defects for 4 weeks. We revealed that nanosecond-pulsed laser treatment for Y-TZP provided a greater degree of BIC than blastedHF-treated Y-TZP. In the case of Ce-TZP, however, laser treatment reduced the BIC compared with blastedHF treatment. Thus, our null hypothesis that nanosecond-pulsed laser treatment improves bone response was accepted for Y-TZP but the second hypothesis that a difference in zirconia did not influence the bone response was rejected.

Generally, a roughened implant surface improves the tissue response. It was reported that a higher degree of implant surface roughness leads to a higher BIC and results in higher implant torque resistance[24]. For titanium implants, the effectiveness of the combination of large grid sandblasted and acid etching treatment is known to enhance bone response[25]. BlastedHF treatment is also useful for enhancing the activity of osteoblast-like cells toward zirconia[11,12]. In the present study, the nanosecond pulsed laser produced microgrooves, the insides of which were nano-scale roughened. We found that nanosecond-pulsed laser treatment was effective for Y-TZP, yielding a higher BIC compared with blastedHF treatment. Confocal laser observation suggested that the laser-treated surface controlled the orientation of new bone apposition. Others have reported that microgrooves approximately 30 μm in width guided osteoblast cellular growth optimally[26,27].

However, laser treatment was not effective for Ce-TZP. For blastedHF treatment, comparable BIC values were obtained for Y-TZP and Ce-TZP. No distinct differences were observed in the surface morphologies between laser/Y-TZP and laser/Ce-TZP. Thus, it is suggested that the surface chemistry after laser irradiation influenced the bone response. After laser irradiation, the surface of Ce-TZP became black. A change in the surface chemistry should be considered.

Heat of several thousand degrees Celsius is imparted to the zirconia surface during nanosecond-pulsed laser irradiation. This heating causes fusion and evaporation on the zirconia surface to create the microgrooves with nano-scale roughened insides[28]. It is supposed that heating by laser irradiation will also cause changes to the atomic population on the zirconia surface. With titanium, laser irradiation produces a thicker oxide layer and greater numbers of OH groups on the surface[15,16]. It was concluded that surface asperities and an OH-group-inclusive oxide layer induced the enhancement of proliferation and cell activity of osteoblasts[16].

For the zirconia surfaces, reduction of oxygen atoms was confirmed by EDX measurement. Comparing Ce-TZP and Y-TZP, Ce-TZP showed a greater degree of reduction of oxygen atoms than Y-TZP after laser irradiation. Ce-TZP has a 30 vol% of Al_2O_3. The thermal conductivity of Al_2O_3 is approximately three to six times higher than that of zirconia[29,30]. Higher thermal conductivity will provide earlier and higher temperature increase after laser irradiation. It is reported that oxygen deficient zirconia is known as black zirconia[31,32]. Thus, it is presumed that laser irradiation to Ce-TZP produced oxygen deficient zirconia on the surface due to the higher temperature after laser irradiation and caused the changing the color of the surface to black. The relationship between the amount of oxygen content on the zirconia surface and BIC is not still clear. However, it is suggested that lesser amount of remaining oxygen may induce less BIC for laser/Ce-TZP. Increasing the availability of oxygen atoms with laser/Ce-TZP will elucidate the influence of oxygen content on bone response. This correlation of oxygen content and bone bonding behavior should be further investigated.

We subcutaneously injected calcein into the rats. Nishikawa *et al.*[33] reported that intravenous injection of calcein produced stronger fluorescent labelling than subcutaneous injection of rat mandible staining. It is presumed that present weak intensities of calcein labeling is due to the subcutaneous injection. Administration intravenous injection of calcein should be further evaluated.

It is reported that sandblasting and grinding of partially stabilized zirconia influences its mechanical properties by phase transformation[18]. Moreover, zirconia substrate may be transformed at any phase by heating. Noda *et al.*[34] reported that Nd:YAG dental laser irradiation induced cracking and reduced the mechanical strength of Y-TZP and Ce-TZP. However, the present study showed no cracks on Y-TZP and Ce-TZP surfaces. This was due to the difference in pulse length of 3 ns in the present study *vs* 5 ms in a previous study reported by Noda *et al.*[34] Detailed studies of phase transformation and methods to preserve the mechanical strengths of Y-TZP and Ce-TZP after laser treatment should be further investigated.

The attachment of gingival connective tissue to implant materials is unsatisfactory compared with its tight bonding to bone. Fukayo *et al.*[17] evaluated the attachment of gingival connective tissue to nanosecond-pulsed laser-treated titanium implants in the rat maxilla. Polarized light microscopic observation revealed perpendicular rod-like attachments of gingival collagen fibers on the laser-treated titanium implant surface. They concluded that a laser treated surface was effective for the perpendicular orientation of collagen fibers that resembled natural human teeth. In our CLSM analysis, new bone formation was orientated perpendicular to the laser-treated surface. The present surface with microgrooves has the potential to control the direction of collagen fibers in soft tissue. The attachment of soft tissue such as gingival connective tissue will be the next subject of our research.

CONCLUSIONS

Nanosecond-pulsed laser irradiation produced microgrooves having insides with nano-scale roughening on Y-TZP and Ce-TZP surfaces. Laser treatment was effective for increasing BIC to Y-TZP, but not to Ce-TZP. We revealed that surface chemistry is one of the factors which will influence the bone formation separately from the surface morphology. Influence of other factors such as crystallographic or electrostatic properties on the bone formation should be further investigated. The present nano-pulsed laser irradiation will be applicable for treatment of zirconia implants.

ACKNOWLEDGMENTS

This work was supported by Grants-in-Aid for Young Scientists (B) (15K20492, 17K17225) and for Scientific Research (C) (17K06074) from the Japan Society for the Promotion of Science, and a Grant-in-Aid from the Society for Tsurumi University School of Dental Medicine (29001). The authors are grateful to R. Yagi and Y. Iinuma for their help with animal experiments.

REFERENCES

1) Wenz HJ, Bartsch J, Wolfart S, Kern M. Osseointergration and clinical success of zirconia dental implants: a systematic review. Int J Prosthodont 2008; 21: 27-36.
2) Andreiotelli M, Wentz HJ, Kohal RJ. Are ceramic implants a viable alternative to titanium implants? A systematic literature review. Clin Oral Implants Res 2009; 20 (Suppl 4): 32-47.
3) Apratim A, Eachempati P, Krishnappa Salian KK, Singh V, Chhabra S, Shah S. Zirconia in dental implantology: A review. J Int Soc Prev Community Dent 2015; 5: 147-156.
4) Hashim D, Cionca N, Courvoisier DS, Mombelli A. A systematic review of the clinical survival of zirconia implants. Clin Oral Investig 2016; 20: 1403-1417.

5) Heydecke G, Kohal R, Gläser R. Optimal esthetics in single-tooth replacement with the Re-Implant system: case report. Int J Prosthodont 1999; 12: 184-189.
6) Valentine-Thon E, Schiwara HW. Validity of MELISA for metal sensitivity testing. Neuro Endocrinol Lett 2003; 24: 57-64.
7) Hirota M, Hayakawa T, Ohkubo C, Sato M, Hara H, Toyama T, Tanaka Y. Bone responses to zirconia implants with a thin carbonate-containing hydroxyapatite coating using a molecular precursor method. J Biomed Mater Res B Appl Biomater 2014; 102: 1277-1288.
8) Att W, Takeuchi M, Suzuki T, Kubo K, Anpo M, Ogawa T. Enhanced osteoblast function on ultraviolet light-treated zirconia. Biomaterials 2009; 30: 1273-1280.
9) Gahlert M, Gudehus T, Elchhom S, Steinhauser E, Kniha H, Erhardt W. Biomechanical and histomorphometric comparison between zirconia implants with varying surface textures and a titanium implant in the maxilla of miniature pigs. Clin Oral Impl Res 2007; 18: 662-668.
10) Schliephake H, Hefti T, Schlottig F, Gédet P, Staedt H. Mechanical anchorage and peri-implant bone formation of surface-modified zirconia in minipigs. J Clin Periodontol 2010; 37: 818-828.
11) Ito H, Sasaki H, Saito K, Honma S, Yajima Y, Yoshinari M. Response of osteoblast-like cells to zirconia with different surface topography. Dent Mater J 2013; 32: 122-129.
12) Hirano T, Sasaki H, Honma S, Furuya Y, Miura T, Yajima Y, Yoshinari M. Proliferation and osteogenic differentiation of human mesenchymal stem cells on zirconia and titanium with different surface topography. Dent Mater J 2015; 34: 872-880.
13) Delgado-Ruíz RA, Calvo-Guirado JL, Moreno P, Guardia J, Gomez-Moreno G, Mate-Sánchez JE, Ramirez-Fernández P, Chiva F. Femtosecond laser microstructuring of zirconia dental implants. J Biomed Mater Res B Appl Biomater 2011; 96: 91-100.
14) Delgado-Ruíz RA, Abboud M, Romanos G, Aguilar-Salvatierra A, Gomez-Moreno G, Calvo-Guirado JL. Peri-implant bone organization surrounding zirconia-microgrooved surfaces circularly polarized light and confocal laser scanning microscopy study. Clin Oral Implants Res 2015; 26: 1328-1337.
15) Honda R, Mizutani M, Ohmori H, Komotori J. Biocompatibility evaluation of nanosecond laser treated titanium surfaces. Int J Mod Phys Conf Ser 2012; 6: 682-687.
16) Mizutani M, Honda R, Kurashina Y, Komotori J, Ohmori H. Improved cytocompatibility of nanosecond-pulsed laser-treated commercially pure Ti surfaces. Int J Auto Tech 2014; 8: 102-109.
17) Fukayo Y, Amemiya T, Nakaoka K, Mizutani M, Komotori J, Hamada Y, Hayakawa T. Bone and gingival connective tissue responses towards nanosecond-pulsed laser-treated titanium implants. J Hard Tissue Biol 2016; 25: 181-194.
18) Sato H, Yamada K, Pezzotti G, Nawa M, Ban S. Mechanical properties of dental zirconia ceramics changed with sandblasting and heat treatment. Dent Mater J 2008; 27: 408-414.
19) Miyazaki T, Nakamura T, Matsumura H, Ban S, Kobayashi T. Current status of zirconia restoration. J Prosthodont Res 2013; 57: 236-261.
20) Ban S, Sato H, Suehiro Y, Nakanishi H, Nawa M. Biaxial flexure strength and low temperature degradation of Ce-TZP/Al_2O_3 nanocomposite and Y-TZP as dental restoratives. J Biomed Mater Res B Appl Biomater 2008; 87: 492-498.
21) Sammons R, Lumbikanonda N, Gross M, Cantzler P. Comparison of osteoblast spreading on microstructured dental implant surfaces and cell behaviour in an explant model of osseointegration: a scanning electron microscopic study. Clin Oral Implants Res 2005; 16: 657-666.
22) Suzuki T, Hayakawa T, Kawamoto T, Gomi K. Bone response of TGF-β2 immobilized titanium in a rat model. Dent Mater J 2014; 33: 233-241.
23) Donath K, Breuner G. A method for study of undecalcified bones and teeth with attached soft tissue: The Säge-Schiff (sawing and grinding) technique. J Oral Pathol Med 1982; 11: 318-326.
24) Shalabi MM, Gortemaker A, Van't Hof MA, Jansen JA, Creugers NHJ. Implant surface roughness and bone healing: a systematic review. J Dent Res 2006; 85: 496-500.
25) Buser D, Schenk RK, Steinemann S, Fiorellini JP, Fox CH, Stich H. Influence of surface characteristics on bone integration of dental implants. A histomorphometric study in miniature pigs. J Biomed Mater Res 1991; 25: 889-902.
26) Delgado-Ruíz RA, Gomez-Moreno G, Aguilar-Salvatierra A, Markovic A, Mante-Sánchez JE, Calvo-Guirado JL. Human fetal osteoblast behavior on zirconia dental implants and zirconia disks with microstructured surfaces. An experimental in vitro study. Clin Oral Implants Res 2016; 27: e144-e153.
27) Puckett S, Pareta R, Webster TJ. Nano rough micron patterned titanium for directing osteoblast morphology and adhesion. Int J Nanomedicine 2008; 3: 229-241.
28) Chaleard C, Detalle V, Kocon S, Lacour JL, Nouvellon C, Mauchien P, Salle B, Semerok A. Experimental investigation of laser ablation efficiency of metal. Proceedings of the SPIE 1998; 3404-432-440.
29) Bansal NP, Zhu D. Thermal conductivity of zirconia-alumina composites. Ceram Int 2005; 31: 911-916.
30) Hostaša J, Pabst W, Matějíček J. Thermal conductivity of Al_2O_3-ZrO_2 composite ceramics. J Am Ceram Soc 2011; 94: 4404-4409.
31) Yoshioka S, Kobayashi Tanaka Y, Yamamoto Y, Miyazaki T. Blackening and crack formation in Q-switched YAG laser machining of zirconia ceramics. J JSPE 1989; 55: 1277-1282.
32) Sinhamahapatra A, Jeon JP, Kang J, Han B, Yu JS. Oxygen-deficient zirconia (ZrO_{2-x}): A new material for solar light absorption. Scientific Reports 2016; 6: 27218.
33) Nishikawa T, Tominaga K, Yun S, Uemura M, Yoshikawa M, Toda T, Tanaka A. Confocal laser scanning microscopy of alveolar bone and dentin in the rat mandible. J Jpn Soc Periodontol 1996; 38: 272-281.
34) Noda M, Okuda Y, Tsuruki J, Minesaki Y, Takenouchi Y, Ban S. Surface damages of zirconia by Nd:YAG dental laser irradiation. Dent Mater J 2010; 29: 536-541.